

WASP: A Weight-Space Approach to Detecting Learned Spuriousness

Cristian Daniel Păduraru^{1,2}Antonio Bărbălău^{1,2}Radu Filipescu^{1,2}Andrei Liviu Nicolicioiu^{3,4}Elena Burceanu¹¹Bitdefender, Romania²University of Bucharest, Romania³Mila, Montreal, Canada⁴University of Montreal, Canada{cpaduraru, ext-abarbalau, rfilipescu, eburceanu}@bitdefender.com
andrei.nicolicioiu@mila.quebec

Abstract

It is of crucial importance to train machine learning models such that they clearly understand what defines each class in a given task. Though there is a sum of works dedicated to identifying the spurious correlations featured by a dataset that may impact the model’s understanding of the classes, all current approaches rely solely on data or error analysis. That is, they cannot point out spurious correlations learned by the model that are not already pointed out by the counterexamples featured in the validation or training sets. We propose a method that transcends this limitation, switching the focus from analyzing a model’s predictions to analyzing the model’s weights, the mechanism behind the making of the decisions, which proves to be more insightful. Our proposed **Weight-space Approach to detecting Spuriousness (WASP)** relies on analyzing the weights of foundation models as they drift towards capturing various (spurious) correlations while being fine-tuned on a given dataset. We demonstrate that different from previous works, our method (i) can expose spurious correlations featured by a dataset even when they are not exposed by training or validation counterexamples, (ii) it works for multiple modalities such as image and text, and (iii) it can uncover previously untapped spurious correlations learned by ImageNet-1k classifiers.



Figure 1: Qualitative results depicting a series of Spurious Correlations (SCs), uncovered employing our proposed WASP approach for CLIP ViT-L/14 [35] fine-tuned on ImageNet-1k [8]. In each scenario, a (real) ImageNet class is depicted alongside a concept found to be positively correlated with a different (predicted) class. Though in every scenarios a single ImageNet-1k class is clearly depicted, the model predicts a class that is not illustrated at all, clinging to the learned SCs.

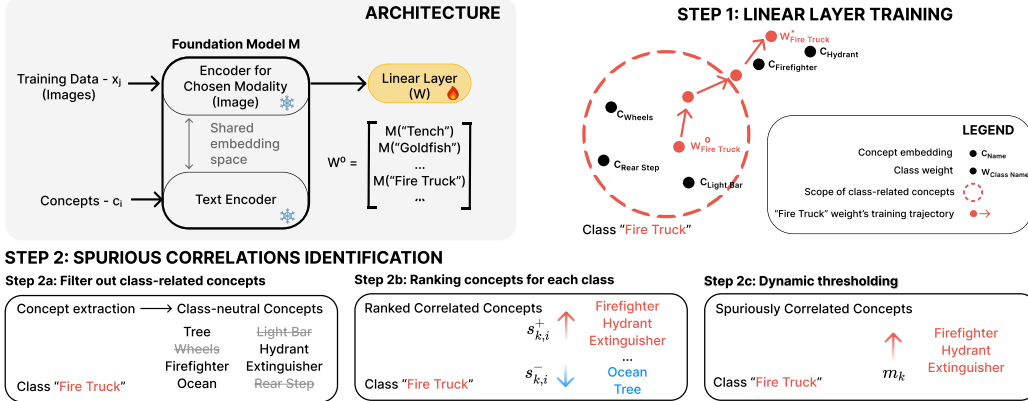


Figure 2: Following WASP’s steps for the ImageNet-1k “Fire Truck” class. In Step 1, during training, the classification weights W drift from the initial class concept embedding W^0 , outside the scope of relevant concepts, towards spuriously correlated ones. In Step 2, our method filters out class-related concepts and, using an embedding-space scoring system, ranks and automatically marks the highest-ranking class-neutral concepts as SCs.

1 Introduction

Deep neural networks, and especially fine-tuned versions of foundation models, are commonly deployed in critical areas such as healthcare, finance, and criminal justice, where decisions based on **spurious correlations (SCs)** can have significant societal consequences [1, 6]. Even if the pretrained model has been validated by the community, the dataset leveraged in the fine-tuning process can, and usually does, imprint the model with new SCs. We present such examples in Fig. 1, where a CLIP model, fine-tuned on ImageNet-1k, labels the first image as a “Fire Truck”, even in the complete absence of any fire truck or truck-related features and even given the presence of a peafowl (which is an ImageNet-1k class) right in front and center. This is due to the fact that, as our proposed WASP protocol discovered, the model spuriously correlates firefighters (which are not an ImageNet-1K class) with the “Fire Truck” class.

Subpopulation shift setups [5, 26, 50], featuring naturally occurring SCs, provide researchers with a controlled environment for studying SC detection and prevention. Within this context, recent efforts have begun to employ foundation models [4, 17, 58] in their investigation protocols. Some of these efforts [4, 58] focused on finding SCs through data analysis, without referencing model predictions. While these findings are valuable, they may not always be relevant. For example, an SC may not impact a machine learning model if the correlation is harder to learn than the actual class itself. To this end, efforts such as that of [17] focused on learned spurious correlations, by investigating validation samples that are misclassified by a model of interest. However, this error-based approach assumes that the validation set is in some sense exhaustive and that the validation samples are already able to expose the SCs learned by the model, which may be true for subpopulation shift setups, but hardly guaranteed in a more general one.

Different from prior work, we aim to overcome the limitations of data and error analysis, revealing spurious correlations learned by machine models even in scenarios in which the training and validation sets do not present counterexamples able to expose the model’s flaws. To this end we propose **WASP**, a Weight-space Approach to detecting learned **Spurious** correlations. Our overall framework is illustrated in Fig. 2 and further detailed in Sec. 3. We leverage the topology of foundation models such as CLIP and mGTE and observe that during the process of training, the weights of the final classification layer drift away from the textual representation of their associated class, towards identifying and prioritizing representations of spurious attributes. We propose a scoring system based on the model’s embedding-space structure to extract concepts that factor in the activation of class neurons and delineate the highest-ranking concepts that lie outside the semantic scope of the classes, as spurious correlation.

Our contributions can be summarized as follows:

1. We introduce **WASP**, a weight-space approach to detecting *learned spuriousness*, offering a departure from the current error or data analysis methodology.
2. We show that our approach surpasses all state-of-the-art methods for *identifying and naming spurious correlations* in a given dataset. First, in its capacity to enhance the robustness of zero-shot models, and second, in its applicability to scenarios lacking spurious correlation counterexamples. Furthermore, in addition to evaluating our method on the established image datasets (Waterbirds, CelebA), we also validate its effectiveness on textual data (CivilComments).
3. We show that our method is able to *expose previously untapped ImageNet-1k spurious correlations*, and further proceed to show that multiple state-of-the-art models are affected by them, highlighting their inability to formulate robust definitions for the targeted classes.

2 Background

Machine learning methods naturally capture relevant factors needed to solve a task. However, models might also capture shortcuts [11], as correlations between non-essential features of the inputs and the label. These shortcuts represent spurious correlations, that don’t hold in a more general setup (*e.g.* using water features to classify waterbirds instead of focusing on the birds’ features), and should not be used for reliable generalization outside the training distribution, as they often lead to degraded performance [34, 3, 13].

SCs from error analysis Approaches like **B2T** [17] rely exclusively on the validation samples, identifying which correlations between concepts are more prevalent in the misclassified examples. To catch SCs, B2T needs samples that oppose the strong correlations in the training set, thus leading to misclassification. To circumvent this limitation, **DrML** [56] manually builds a list of texts containing classes and concepts associations, that could potentially underline an SC. It forwards each such textual association through a classifier, learned on the image modality, and keeps as SCs the erroneously classified ones. In those approaches, the burden falls on the practitioners to come up with exhaustive samples or associations, failing to detect unexpected SCs. Differently, **WASP** focuses on analyzing the explicit learned weights of a model, covering all trainset samples. We thus extract the spuriously correlated concepts directly from the weights, bypassing the need for an exhaustive validation set or correlations candidates.

SCs from train data analysis In **SpLiCE** [4] each image is decomposed into high-level textual concepts, searching next for concepts that are frequent for a certain class, but not for the others. **LG** [58] relies on LLMs to propose concepts potentially correlated with each class, using image captions. Next, it uses CLIP [35] to estimate a class-specificity score for each concept, and highly scored concepts for a class *w.r.t.* the others are considered SCs. These methods focus on the concepts’ occurrences per class, making them prone to missing low-frequency concepts, as their presence can be drowned when averaging scores over a large dataset. Moreover, the SCs found through data analysis could be harder to learn than the class itself, so they are not necessarily imprinted in the model. In contrast, learned SCs (including error analysis revealed ones) must always be addressed, as they are, by definition, proven to impact the classifier. For this reason, **WASP** targets learned SCs by looking directly at the impact of the training set upon the model’s weights.

Manual interpretation of correlations The method introduced in [41] finds spurious features learned by a model, but it requires humans to manually annotate whether an image region is causal or not for a class. While this ensures a higher quality of the annotations, it also poses problems of scalability to large datasets. In contrast, **WASP** works fully automated, at scale, identifying SCs for each class in ImageNet-1k.

SCs from subpopulation shift setup Other previous works [33, 23, 2, 54] have focused on SC identification strictly within the context of subpopulation shifts. The particularity of this setup is that the training and validation sets always contain subsets of samples that oppose the strong spurious correlations of the dataset. Most of these methods [33, 23, 54] focus on first learning a strongly biased classifier and then either separate the samples of each class into two groups [33, 54] (one containing correctly classified examples and the other containing misclassified ones), or place higher weights on hard samples [23], in order to balance the dataset. **CoBaIT** [2] on the other hand uses an

unsupervised method for object recognition and then samples the dataset examples such that all object types are uniformly distributed in each class. Their result contains heatmaps overlays on images, which can offer insights to guide further manual SCs identification. Some of the most commonly used datasets in this setup are Waterbirds [37], CelebA [26] and CivilComments [5].

Preventing the learning of SCs As the statistical correlation of attributes and classes lies at the root of learning SCs, breaking this correlation is an accessible way of preventing their learning. Assuming that the training set features all combination of classes and attributes, this can be achieved by balancing all the existing groups of samples, as defined by the intersection of class and attribute labels. **GroupDRO** [37] uses group-specific weights that are dynamically updated during training to balance them, and it is the approach most commonly taken by works that simply find dataset partitions [33, 54], and also by works that name the SCs, and then obtain pseudo-labels for those attributes [17, 58]. To judge the robustness of a classifier, the **worst-group accuracy** metric is employed, which computes the accuracy on each individual group of samples and then reports their minimum. The worst-group accuracy of GroupDRO with ground truth attribute labels is usually viewed by the previously mentioned works as an upper bound on the performance that can be obtained.

3 Our Method

For a standard classification task, we aim to identify spurious correlations learned by a model through training on a new dataset. By **dataset’s SCs** we refer to class-independent concepts, whose presence in the samples greatly affects the class label distribution. By **concepts** we refer to words or expressions with a well-defined semantic content. Through **SCs learned by a classifier** f_θ we refer to concepts causally unrelated with a class, whose presence in the input significantly changes the distribution of class probabilities predicted by f_θ . We further classify them as positively correlated concepts w.r.t. to a class k , if their presence in the input increases the probability of f_θ predicting the class k , and negatively correlated concepts if they decrease it.

Setup We start with a dataset of samples $(x_j, y_j) \in (\mathcal{X}, \mathcal{Y})$ and construct the set of concepts $c_i \in C_{all}$ in textual form, that are present in the training data. We use a foundation model M , capable of embedding both the input samples x_j and the concepts c_i in aligned representations in \mathbb{R}^D . The main steps of our method (also revealed in Fig. 2, and in more detail in the Alg. 3.1), are the following:

Initialization We train a linear layer on top of the embedding space from M . We initialize w_k , the weights of class k in this layer, with the embedding of its corresponding class name, extracted by the model M :

$$w_k^0 = M(\text{class_name}_k), k \in \overline{1, |K|}, \quad (1)$$

where K is the list of class names.

Step 1: Model training We train the weights of the linear layer using ERM [48]. Through learning, the weights for each class k in the linear layer naturally shift from their original initialization, $M(\text{class_name}_k)$, towards w_k^* , as visually presented in Fig. 2.

Step 2: SCs identification Since the weights w_k and concepts c_i share the same embedding space, we continue by identifying which concepts c_i are correlated with each class k , as follows:

a. Filter out class-related concepts After extracting c_i concepts present in the dataset using existing tools, we filter out the concepts that are related to any actual class, leaving only concepts that are causally unrelated to all classes, which

we call **class-neutral concepts**. We argue that only these concepts are proper candidates for SCs, as they are not required nor useful for the robust recognition of a class (e.g. a forest background is well correlated with species of landbirds, but we want to prevent the model from relying on this

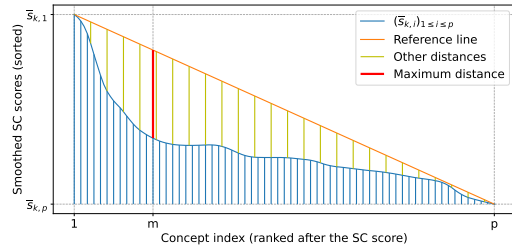


Figure 3: The maximum distance between the reference line and the smoothed scores gives the threshold for our cut-off heuristic.

correlation, which is causally unrelated w.r.t. the class definition). The exact pipeline and tools for processing the concepts (extraction and filtering) are detailed in Sec. 4.

b. Rank class-neutral concepts For each class-neutral concept c_i and class k , we rank the concepts based on their similarities with the learned class weights w_k^* , using the following positive-SC score:

$$s_{k,i}^+ = w_k^{*\top} M(c_i) - \min_{k' \in 1, |K|} w_{k'}^{*\top} M(c_i). \quad (2)$$

Intuitively, we want concepts similar to one class but not to all the others. Thus, for each class k , we select the concepts which starkly correlate to it, compared to all other classes. For the negatively correlated SCs, $s_{k,i}^-$ we use the dissimilarity score: $-w_k^{*\top} M(c_i)$.

c. Dynamic thresholding We next keep only the highest-ranked SCs of each class, using a *dynamic threshold* for the scores above, that allows us to automatically select the SCs for each class. To smooth the curve of scores, we apply a mean filter on top of the ranked concepts (window size r). We denote the scores obtained at this step with $(\bar{s}_{k,i})_{1 \leq i \leq p}$, with $p = q - r + 1$, where q is the total number of filtered concepts. We then select the top m_k ones, as positive SCs for class k , where the m_k index is defined as:

$$m_k = \lfloor r/2 \rfloor + \arg \max_i \left(\bar{s}_{k,1} - i \frac{\bar{s}_{k,1} - \bar{s}_{k,p}}{p-1} - \bar{s}_{k,i} \right). \quad (3)$$

The intuition is that m_k represents the index where the curve of smoothed scores, $\bar{s}_{k,i}$, deviates the most from the straight reversed diagonal line, connecting $\bar{s}_{k,1}$ and $\bar{s}_{k,p}$, like visually shown in Fig. 3.

3.1 Algorithm

We present the pseudocode of our proposed WASP approach in Alg. 1. We annotate the main steps presented in Sec. 3. At line 1, we initialize the class weights of our linear probing layer with the text embeddings of the class names, the zero-shot classification weights of the foundation model M . We then fine-tune the layer (line 2), on the given dataset. At lines 3-4, we filter the list of concepts and compute the embeddings for the remaining class-neutral concepts. The filtering can be performed by means of employing WordNet associations, Large Language Models, or both, as described in Sec. 4. With the embeddings of the class-neutral concepts at hand, we proceed to determine the SCs for each class. At line 5, we initialize our set of spuriously correlated concepts with an empty set, and we compute the similarities between each selected concept and each class at line 6. Next, for each class k , we compute the set of scores for all concepts w.r.t. this class and store it in s_k (line 8). For each class-neutral concept, its ranking score for the current class is the difference between its similarity to the current class and the smallest similarity with a different class. Lines 9-11 formally implement the dynamic thresholding procedure, described in Sec. 3. Finally, we select the top concepts (above the computed threshold m_k) and store them as spuriously correlated concepts for class k (lines 12-13).

4 Experimental Setup

Foundation models (FM) We used mGTE (gte-large-en-v1.5 [55]) for text embeddings in CivilComments [5], and OpenAI CLIP ViT-L/14 [35] for text and images otherwise.

Concept extraction For the image classification task, we first use the GIT-Large [51] captioning model (trained on MSCOCO [22]) to obtain descriptions of the dataset’s images. Next, we extract concepts from the captions (or directly from the text samples for the text classification task), using YAKE [7] keyword extractor, taking the top 256 n-grams for $n = 3, 5$.

Concepts filtering We use Llama-3.1-8B-Instruct [10] to remove class instances from the concepts extracted at the previous step. We also apply a post-processing based on WordNet [30] to catch obvious class instances that the LLM might miss. For each class we specify a word used to search for synsets in the WordNet [30] hierarchy (e.g. *bird* for Waterbirds) and then remove individual words that match with any hyponym or hypernym of those synsets.

Training We train the linear layer on L_2 normalized embeddings extracted by the FM, using PyTorch’s [32] AdamW [28] optimizer with a learning rate of $1e-4$, weight decay of $1e-5$ and batch size of 1024. We use the cross entropy loss with balanced class weights as the objective. The weights of the layer are normalized after each update and we use CLIP’s [35] temperature to scale the logits. We use the validation set’s class-balanced accuracy for model selection and early stopping.

Algorithm 1 WASP - Weight space Approach to detecting learned SPuriousness

Input: M - foundation model with associated text encoder; $(\mathcal{X}, \mathcal{Y})$ - Training set; $(\mathcal{X}_{val}, \mathcal{Y}_{val})$ - Validation set; K - list of class names; C_{all} - list of all concepts; r - window for dynamic thresholding.

Output: Identified positive SCs: \mathcal{B} .

```

1:  $\mathbf{W}^0 \leftarrow M(K)$ 
2:  $\mathbf{W} \leftarrow \text{ERM}(\mathbf{W}^0, M, (\mathcal{X}, \mathcal{Y}), (\mathcal{X}_{val}, \mathcal{Y}_{val}))$  ▷ 1. Model Training
3:  $C \leftarrow \text{Filter}(C_{all})$  ▷ 2a. Filter concepts: LLM/WordNet
4:  $\mathbf{C}^* \leftarrow M(C)$ 
5:  $\mathcal{B} \leftarrow \emptyset$ 
6:  $\mathbf{S} \leftarrow \mathbf{W}^\top \mathbf{C}^*$  ▷ 2b. Rank class-neutral concepts
7: for  $k \in \overline{1, |K|}$  do
8:    $s_k = [\mathbf{S}_{k,j} - \min_{k' \in \overline{1, |K|}} \mathbf{S}_{k',j}, \text{ for all } j \in \overline{1, |C|}]$  ▷ 2c. Dynamic thresholding
9:    $\bar{s}_k = \text{mean\_pool}(\text{reversed}(\text{sorted}(s_k)), r)$ 
10:   $p = |C| - r + 1$ 
11:   $m_k = \lfloor r/2 \rfloor + \arg \max_i \left( \bar{s}_{k,1} - i \frac{\bar{s}_{k,1} - \bar{s}_{k,p}}{p-1} - \bar{s}_{k,i} \right)$ 
12:   $b_k = [s_{k,i} \mid i \leq m_k]$ 
13:   $\mathcal{B} = \mathcal{B} \cup (k, b_k)$  ▷ Positive SCs
14: end for

```

4.1 Datasets

Waterbirds [37] is a common dataset for generalization and mitigating spurious correlations. It is created from CUB [49], by grouping species of birds into two categories, *landbirds* and *waterbirds*, each one being spuriously correlated with the background, land, and water respectively.

CelebA [26] is a large-scale collection of celebrity images (over 200,000), widely used in computer vision research. For generalization context, the setup [27] consists of using the *Blond_Hair* attribute as the class label and the *gender* as the spurious feature.

CivilComments [5] is a large collection of 1.8 million online user comments. This dataset is used employed in NLP bias and fairness research concerning different social and ethnical groups.

ImageNet-1k [8] is a larger-scale popular dataset for image classification (1000 classes, with approx. 1300 training samples and 50 validation samples per class).

Table 1: SC-enhanced zero-shot prompts. Following B2T [17], we explicitly introduce the SCs in the prompting scheme of the Foundational Models, leveraging that a more complete description of the image aids the zero-shot classification process. We note that using SCs identified by WASP significantly improves the worst group accuracy across all datasets (image and text modalities).

	Waterbirds	CelebA	CivilComm			
	(Acc % \uparrow)	(Acc % \uparrow)	(Acc % \uparrow)			
Zero-shot	Worst	Avg.	Worst	Avg.	Worst	Avg.
Basic	35.2	84.2	72.8	87.7	33.1	80.2
w B2T	48.1	86.1	72.8	88.0	-	-
w SpLiCE	48.1	82.5	67.2	90.2	-	-
w Lg	46.1	85.9	50.6	87.2	-	-
w WASP	50.3	86.3	73.1	85.7	53.2	71.0

5 Evaluating spurious correlations

For a proper quantitative evaluation of our proposed SCs, beyond the subjectivity of the qualitative aspects, we combine the concepts identified by **WASP** with different components: in Sec. 5.1 we use SC-enhanced prompts for zero-shot classification with a FM; in Sec. 5.2 we evaluate using scenarios lacking spurious correlation counterexamples; and in Sec. 5.4 we generate samples exploiting the discovered concepts; An extended list of the extracted concepts can be found in Appx. F.

5.1 Spurious-aware zero-shot prompting

To further validate our identified spurious correlations, we follow [17] and evaluate them in the context of a zero-shot classification task. We augment the initial, class-oriented prompt with the identified concepts through a *minimal* intervention (e.g. 'a photo of a {cls} in the {concept}') (see Appx. G). For each class we create a prompt with each identified spurious correlation. When classifying an image, we take into account only the highest similarity among the prompts of a class

Table 2: Learning in the context of perfect spurious correlations. In the absence of samples that associate a class instance and concepts spuriously correlated with other classes, GroupDRO does not outperform the standard ERM. In contrast, our regularization based on the identified concepts consistently yields improvements (concerning worst group accuracy) over the considered baselines: ERM, GroupDRO, and the regularization with random causally unrelated concepts (obtained after the filtering in Step2a).

Method	Waterbirds (Acc % \uparrow)		CelebA (Acc % \uparrow)		CivilComments (Acc % \uparrow)	
	Worst	Avg.	Worst	Avg.	Worst	Avg.
ERM [48]	43.2 \pm 5.7	72.7 \pm 2.2	9.6 \pm 1.0	58.2 \pm 0.4	18.6 \pm 0.3	49.9 \pm 0.2
GroupDRO [37]	38.9 \pm 5.4	71.2 \pm 2.0	8.1 \pm 0.3	60.3 \pm 1.0	18.7 \pm 0.4	50.2 \pm 0.5
Regularize w/ random SCs	46.6 \pm 2.7	75.3 \pm 1.1	9.4 \pm 0.0	61.4 \pm 2.0	19.1 \pm 1.6	50.8 \pm 0.9
Regularize w/ Lg's SCs [58]	50.4 \pm 0.1	76.6 \pm 0.0	8.3 \pm 0.0	61.2 \pm 0.5	-	-
Regularize w/ WASP 's SCs	57.9 \pm 0.3	79.8 \pm 0.1	10.4 \pm 0.5	62.0 \pm 1.8	31.3 \pm 0.7	57.5 \pm 0.4

(zero-shot with max-pooling over prompts). See in Tab. 1 how the SCs revealed by our method improve the worst group accuracy over the initial zero-shot baseline and other state-of-the-art solutions, in all the tested datasets. This highlights the relevance of the SCs automatically extracted by WASP. See more ablation experiments in Appx. H.

5.2 Training in a Fully Spurious Setup

We explore here an extreme setup, featuring no spurious correlation counterexample. In real world, this might be the case for most of the SCs, since usually this kind of correlations are generated by decisions in dataset acquisitions and filtering. Removing the minority groups from common robustness datasets, renders GroupDRO-like approaches completely ineffective, as their performance at best only matches the standard ERM (see Tab. 2). We use the employed SCs to impose a regularization upon the trained linear probes, learned on top of frozen embeddings from the FM. Intuitively, we constraint the weights to be equally distanced from the identified SCs. We formulate this as an MSE between the similarity of class weight w_k with an SC b and the average similarity of all class weights with b , these terms being scaled by τ (CLIP's temperature):

$$\mathcal{L}_{reg}(b) = \frac{\tau^2}{N} \sum_{k=1}^N \left[w_k^\top M(b) - sg \left(\frac{1}{N} \sum_{j=1}^N w_j^\top M(b) \right) \right]^2, \quad (4)$$

with sg being the stop gradient operator. The final loss is $\mathcal{L} = \mathcal{L}_{ERM} + \alpha \frac{1}{|\mathcal{B}|} \sum_{b \in \mathcal{B}} \mathcal{L}_{reg}(b)$, where \mathcal{B} is the set of selected concepts and $\alpha = 0.1$. In Tab. 2, we present the results of linear probing with this loss, in the previously mentioned scenario, with no SC counterexamples, just 100% correlations between chosen tuples of concepts and classes. Through SC regularization, the learned classification weights are less reliant on the revealed SCs. The improvement in worst group accuracy shows the new representations are more robust and better aligned with the classification task, underling that WASP identifies concepts that are truly spuriously correlated with the classes. For a better comparison, we replicate the SC identification process of Lg [58] in this scenario.

5.3 Qualitative examples

We present in Tab. 3 the concepts identified as spuriously correlated with each class by WASP and competitors. Notice how our method discovers many new concepts (in blue) when compared with others. This is because our approach is fundamentally different, as it relies on the decision-making process of the model being investigated, diverging from current techniques oriented to validation set errors (B2T), or others that do data analysis over frozen concepts (SpLiCE, Lg). For CelebA-*blonde hair*, B2T and WASP do not find any SCs. This turn out to be an appropriate decision, since the presence of the feminine features do not incline the model towards one class or the other. See an exhaustive list of SCs revealed by WASP (ImageNet-1k included) in Appx. F.

Table 3: Qualitative SCs examples, extracted on Waterbirds, CelebA and CivilComments datasets. See in **red** concepts that are off-topic, person names, or too related to the semantic content of the class, and in **blue** new concepts, that were not identified before. WASP, w.r.t. others, focus on learned SCs, discovering many new spuriously correlated concepts (and expressions, marked with ...).

	Waterbirds		CelebA		CivilComments	
	<i>landbird</i>	<i>waterbird</i>	<i>blonde hair</i>	<i>non-blonde hair</i>	<i>offensive</i>	<i>non-offensive</i>
B2T [17]	forest, woods, tree, branch	ocean, beach, surfer, boat, dock, water, lake	-	man, male	-	-
SpLiCE [4]	bamboo, perched, rainforest	flying	hairstyles, dolly, turban, actress, tennis, beard	hairstyles, visor, amy, kate, fielder, cuff, rapper, cyclist	-	-
Lg [58]	forest, woods, rainforest, tree branch, tree	beach, lake, water, seagull, pond	...blonde hair, actress, model, woman long hair	man..., sunglasses, young man, black hair, actor	-	-
WASP (ours)	forest..., bamboo..., ground, field, log, grass..., tree	swimming..., water, lake, flying..., boat, lifeguard, pond	-	hat..., man..., actor, person, dark, large, shirt	hypocrisy, allowing, troll, solly, hate	work, made, talk

Table 4: Results for three positively correlated SCs found using WASP for CLIP ViT-L/14 fine-tuned on ImageNet. We evaluate the model’s capability to recognize a depicted (correct) class before and after the introduction of an identified concept in the image. For each prompt, 1000 images are generated using FLUX.1-dev. We observe throughout all considered scenarios, a significant drop in the model’s capacity to identify the correct class when the selected concept is involved and a large increase in the likelihood of having the induced class predicted even though it is not illustrated.

Correct Class	Exploited SC (Induced Class)	Prompt	Samples Predicted As (%)	
			Correct Class	Induced Class
peafowl	firemen (fire truck)	• a photo of a peafowl • firemen and a peafowl	100.0 5.3 (-94.7)	0.0 93.4 (+93.4)
Mexican hairless dog	reading a newspaper (crossword)	• a photo of a Mexican hairless dog • a man reading a newspaper in a chair with a Mexican hairless dog in his lap	47.5 0.9 (-46.6)	0.0 36.6 (+36.6)
Bernese Mountain Dog	shrimp (American lobster)	• a photo of a Bernese Mountain Dog • shrimp and pasta near a Bernese Mountain Dog	99.8 10.6 (-89.2)	0.0 37.2 (+37.2)

5.4 ImageNet Spurious Correlations

In the previous subsections we have shown that our proposed method exhibits the desired behavior in the controlled setups popular within the subpopulation shift literature aimed at identifying and preventing spurious correlations. We have also shown that the SCs found by our method aid in improving the zero-shot performance of CLIP, outperforming existing approaches, and that WASP is applicable to situations which lie outside the scope of existing approaches, namely: (i) it is applicable in scenarios in which the training data features 100% spuriously correlated samples, with no counterexamples to point out the SCs, and (ii) it is applicable to both image and text datasets.

Within this subsection, we venture even further and apply our method in an uncontrolled, general setup. Specifically, we employ WASP to point out spurious correlations plaguing the decision-making process of OpenAI’s CLIP ViT-L/14 fine-tuned on ImageNet. Within the ImageNet setup, the current state-of-the-art approach, B2T [17], points out the SCs learned by the model by analyzing the mistakes the model makes when evaluated on the validation set. Different from B2T [17], our approach does not rely on the validation data to provide counterexamples able to expose the SCs, and it is able to provide a list of SCs which exceeds the scope of the validation dataset. We provide extensive lists of SCs pointed out by our method in Appx. F. We note that most of the SCs pointed out by our method are previously untapped, opening up a new avenue for investigating ImageNet SCs.

Table 5: Accuracy of various convolutional and transformer-based models trained on ImageNet-1k, on the data generated for Tab. 4. As with Fig. 1, we note that the performance of these models is significantly affected, even though the correct class is illustrated right in front and center while the predicted class is absent from the generated images. An exhaustive list is presented in Appx. I.

Model	Prompt employed (correct class highlighted in bold and blue , SC in yellow)				
	a photo of a peafowl	firemen and a peafowl	a photo of a Bernese Mountain Dog	shrimp and pasta near a Bernese Mountain Dog	
alexnet [19]	100.0	4.6 (-95.4)		96.2	23.3 (-72.9)
efficientnet_b1 [45]	100.0	42.6 (-57.4)		88.1	67.1 (-21.0)
regnet_x_32gf [36]	100.0	66.1 (-33.9)		85.9	46.0 (-39.9)
resnet50 [12]	100.0	30.1 (-69.9)		73.9	54.5 (-19.4)
resnext101_32x8d [52]	100.0	66.6 (-33.4)		84.7	61.2 (-23.5)
squeezezenet1_1 [16]	100.0	13.8 (-86.2)		91.2	46.1 (-45.1)
swin_b [24]	100.0	81.5 (-18.5)		95.2	72.6 (-22.6)
vgg19_bn [40]	100.0	35.9 (-64.1)		83.1	46.2 (-36.9)
vit_l_16 [9]	100.0	55.9 (-44.1)		95.3	76.0 (-19.3)
wide_resnet50_2 [53]	100.0	60.6 (-39.4)		95.7	63.9 (-31.8)

We further invest the effort to generate and manually verify images in order to open up this avenue and showcase previously undiscovered flaws in state-of-the-art models. To this end, we employ a quantized version of FLUX.1-dev [20], and in order to validate the impact of the SCs, we prompt the generative model to depict a chosen (correct) class alongside a non-ImageNet object that we identified as a positive SC for a different class.

The validation process is presented for three distinct scenarios in Tab. 4. Each scenario is defined by a correct class that is illustrated in the image, a concept (object, property, or activity) that is not causally tied to any class, and an absent class *induced* through the presence of the concept. We expect the classifier to predict this absent class, based on our scoring. We measure the impact of the concept by comparing the model’s ability to predict the correct class before and after its introduction. We generate and manually ensure the compliance of 1000 images for each scenario and we evaluate the model both in terms of accuracy and in terms of the frequency with which it predicts the induced class. Throughout all considered scenarios, we observe a significant drop in the model’s capacity to identify the correct class when the SC factor is involved, with an increased likelihood of having the induced class predicted, even though it is not illustrated in any way, shape or form in the image.

Within the same context, we present a series of qualitative examples in Fig. 1. We emphasize that, even though throughout most of these samples, a single ImageNet-1k class is clearly depicted, the model chooses to ignore it and label the image as a completely different class, not illustrated at all in the image, solely based on the presence of a non-ImageNet object. We underline, by means of the results presented in Tab. 4, that the model is not fooled by artifacts in the generated images to predict randomly. We test the performance of the models on images featuring the correct class, without added objects. We observe this way that the model’s performance on the generated data is on par with the original performance of the model on these classes, validating that the generated images are not out of distribution. Furthermore, we show that the rate at which the induced class is predicted increases significantly.

The model at hand is generally considered to be a robust state-of-the-art model, benefiting from ample pre-training. We emphasize through our experiment that even under these reassuring circumstances, critical reasoning flaws can make their way through, in a production-ready model, undetected by validating and examining the model’s performance on held-out data. We further proceeded to examine the impact of the SCs for which we have generated data on an exhaustive set of ImageNet-1k state-of-the-art models. We present the entire set of results in Appx. I, and the results for a selection of these models in Tab. 5. We emphasize that, even large transformer models, such as ViT-L/16 are heavily influenced by learned SCs. These results thus showcase the generality of our findings and the major impact that SCs silently had on state-of-the-art models.

6 Conclusions

We introduce **WASP**, a method that automatically identifies SCs through a weight-space analysis that can be scaled to large datasets. We have evaluated our approach on existing benchmarks, showcasing the relevancy of the proposed SCs, while proving that, different from existing work: (i) our method is applicable to both text and image datasets and that (ii) it is applicable in scenarios featuring fully spuriously correlated samples. Furthermore, using our method we have discovered previously untapped ImageNet SCs and showed that they affect multiple state-of-the-art models.

References

- [1] Angwin, Julia and Larson, Jeff and Mattu, Surya and Kirchner, Lauren. Machine Bias. There’s software used across the country to predict future criminals. And it’s biased against blacks. <https://www.propublica.org/article/machine-bias-risk-assessments-in-criminal-sentencing>, 2016. Accessed on: 2024-08-31.
- [2] Md Rifat Arefin, Yan Zhang, Aristide Baratin, Francesco Locatello, Irina Rish, Dianbo Liu, and Kenji Kawaguchi. Unsupervised concept discovery mitigates spurious correlations. In Ruslan Salakhutdinov, Zico Kolter, Katherine Heller, Adrian Weller, Nuria Oliver, Jonathan Scarlett, and Felix Berkenkamp, editors, *Proceedings of the 41st International Conference on Machine Learning*, volume 235 of *Proceedings of Machine Learning Research*, pages 1672–1688. PMLR, 21–27 Jul 2024.
- [3] Sara Beery, Grant Van Horn, and Pietro Perona. Recognition in terra incognita. In *Proceedings of the European conference on computer vision (ECCV)*, 2018.
- [4] Usha Bhalla, Alex Oesterling, Suraj Srinivas, Flavio Calmon, and Himabindu Lakkaraju. Interpreting clip with sparse linear concept embeddings (splice). *Advances in Neural Information Processing Systems*, 37:84298–84328, 2024.
- [5] Daniel Borkan, Lucas Dixon, Jeffrey Sorensen, Nithum Thain, and Lucy Vasserman. Nuanced Metrics for Measuring Unintended Bias with Real Data for Text Classification. *CoRR*, abs/1903.04561, 2019.
- [6] Aylin Caliskan, Joanna J. Bryson, and Arvind Narayanan. Semantics derived automatically from language corpora contain human-like biases. *Science*, 356(6334):183–186, 2017.
- [7] Ricardo Campos, Vítor Mangaravite, Arian Pasquali, Alípio Jorge, Célia Nunes, and Adam Jatowt. YAKE! Keyword extraction from single documents using multiple local features. *Information Sciences*, 509:257–289, 2020.
- [8] Jia Deng, Wei Dong, Richard Socher, Li-Jia Li, Kai Li, and Li Fei-Fei. ImageNet: A large-scale hierarchical image database. In *IEEE Computer Society Conference on Computer Vision and Pattern Recognition CVPR*, 2009.
- [9] Alexey Dosovitskiy, Lucas Beyer, Alexander Kolesnikov, Dirk Weissenborn, Xiaohua Zhai, Thomas Unterthiner, Mostafa Dehghani, Matthias Minderer, Georg Heigold, Sylvain Gelly, Jakob Uszkoreit, and Neil Houlsby. An image is worth 16x16 words: Transformers for image recognition at scale. In *9th International Conference on Learning Representations, ICLR 2021, Virtual Event, Austria, May 3-7, 2021*. OpenReview.net, 2021.
- [10] Abhimanyu Dubey, Abhinav Jauhri, Abhinav Pandey, Abhishek Kadian, Ahmad Al-Dahle, Aiesha Letman, Akhil Mathur, Alan Schelten, Amy Yang, Angela Fan, et al. The llama 3 herd of models. *arXiv preprint arXiv:2407.21783*, 2024.
- [11] Robert Geirhos, Jörn-Henrik Jacobsen, Claudio Michaelis, Richard Zemel, Wieland Brendel, Matthias Bethge, and Felix A Wichmann. Shortcut learning in deep neural networks. *Nature Machine Intelligence*, 2(11):665–673, 2020.
- [12] Kaiming He, Xiangyu Zhang, Shaoqing Ren, and Jian Sun. Deep residual learning for image recognition. In *2016 IEEE Conference on Computer Vision and Pattern Recognition, CVPR 2016, Las Vegas, NV, USA, June 27-30, 2016*, pages 770–778. IEEE Computer Society, 2016.

[13] Dan Hendrycks, Kevin Zhao, Steven Basart, Jacob Steinhardt, and Dawn Song. Natural adversarial examples. In *Proceedings of the IEEE/CVF Conference on Computer Vision and Pattern Recognition*, pages 15262–15271, 2021.

[14] Andrew Howard, Ruoming Pang, Hartwig Adam, Quoc V. Le, Mark Sandler, Bo Chen, Weijun Wang, Liang-Chieh Chen, Mingxing Tan, Grace Chu, Vijay Vasudevan, and Yukun Zhu. Searching for MobileNetV3. In *2019 IEEE/CVF International Conference on Computer Vision, ICCV 2019, Seoul, Korea (South), October 27 - November 2, 2019*, pages 1314–1324. IEEE, 2019.

[15] Gao Huang, Zhuang Liu, and Kilian Q. Weinberger. Densely connected convolutional networks. *CoRR*, abs/1608.06993, 2016.

[16] Forrest N. Iandola, Matthew W. Moskewicz, Khalid Ashraf, Song Han, William J. Dally, and Kurt Keutzer. SqueezeNet: Alexnet-level accuracy with 50x fewer parameters and <1mb model size. *CoRR*, abs/1602.07360, 2016.

[17] Younghyun Kim, Sangwoo Mo, Minkyu Kim, Kyungmin Lee, Jaeho Lee, and Jinwoo Shin. Discovering and Mitigating Visual Biases through Keyword Explanation. In *CVPR*, 2024.

[18] Pang Wei Koh, Thao Nguyen, Yew Siang Tang, Stephen Mussmann, Emma Pierson, Been Kim, and Percy Liang. Concept bottleneck models. In *International conference on machine learning*, pages 5338–5348. PMLR, 2020.

[19] Alex Krizhevsky. One weird trick for parallelizing convolutional neural networks. *CoRR*, abs/1404.5997, 2014.

[20] Black Forest Labs. FLUX by Black Forest Labs. <https://github.com/black-forest-labs/flux>, 2024. Accessed on: 2024-11-13.

[21] Weixin Liang, Yuhui Zhang, Yongchan Kwon, Serena Yeung, and James Y. Zou. Mind the gap: Understanding the modality gap in multi-modal contrastive representation learning. In *Advances in Neural Information Processing Systems 35: Annual Conference on Neural Information Processing Systems, NeurIPS*, 2022.

[22] Tsung-Yi Lin, Michael Maire, Serge J. Belongie, James Hays, Pietro Perona, Deva Ramanan, Piotr Dollár, and C. Lawrence Zitnick. Microsoft COCO: Common Objects in Context. In *ECCV*, 2014.

[23] Evan Z Liu, Behzad Haghgoo, Annie S Chen, Aditi Raghunathan, Pang Wei Koh, Shiori Sagawa, Percy Liang, and Chelsea Finn. Just train twice: Improving group robustness without training group information. In Marina Meila and Tong Zhang, editors, *Proceedings of the 38th International Conference on Machine Learning*, volume 139 of *Proceedings of Machine Learning Research*, pages 6781–6792. PMLR, 18–24 Jul 2021.

[24] Ze Liu, Yutong Lin, Yue Cao, Han Hu, Yixuan Wei, Zheng Zhang, Stephen Lin, and Baining Guo. Swin transformer: Hierarchical vision transformer using shifted windows. In *2021 IEEE/CVF International Conference on Computer Vision, ICCV 2021, Montreal, QC, Canada, October 10-17, 2021*, pages 9992–10002. IEEE, 2021.

[25] Zhuang Liu, Hanzi Mao, Chao-Yuan Wu, Christoph Feichtenhofer, Trevor Darrell, and Saining Xie. A convnet for the 2020s. In *IEEE/CVF Conference on Computer Vision and Pattern Recognition, CVPR 2022, New Orleans, LA, USA, June 18-24, 2022*, pages 11966–11976. IEEE, 2022.

[26] Ziwei Liu, Ping Luo, Xiaogang Wang, and Xiaoou Tang. Deep Learning Face Attributes in the Wild. In *2015 IEEE International Conference on Computer Vision (ICCV)*, pages 3730–3738, 2015.

[27] Ziwei Liu, Ping Luo, Xiaogang Wang, and Xiaoou Tang. Deep Learning Face Attributes in the Wild. In *Proceedings of International Conference on Computer Vision (ICCV)*, December 2015.

[28] Ilya Loshchilov and Frank Hutter. Decoupled Weight Decay Regularization, 2019.

[29] Ningning Ma, Xiangyu Zhang, Hai-Tao Zheng, and Jian Sun. ShuffleNet V2: Practical Guidelines for Efficient CNN Architecture Design. In Vittorio Ferrari, Martial Hebert, Cristian Sminchisescu, and Yair Weiss, editors, *Computer Vision - ECCV 2018 - 15th European Conference, Munich, Germany, September 8-14, 2018, Proceedings, Part XIV*, volume 11218 of *Lecture Notes in Computer Science*, pages 122–138. Springer, 2018.

[30] George A. Miller. WordNet: a lexical database for English. *Commun. ACM*, 38(11):39–41, nov 1995.

[31] Tuomas Oikarinen, Subhro Das, Lam M Nguyen, and Tsui-Wei Weng. Label-free concept bottleneck models. *arXiv preprint arXiv:2304.06129*, 2023.

[32] Adam Paszke, Sam Gross, Soumith Chintala, Gregory Chanan, Edward Yang, Zachary DeVito, Zeming Lin, Alban Desmaison, Luca Antiga, and Adam Lerer. Automatic differentiation in pytorch. In *NIPS 2017 Workshop on Autodiff*, 2017.

[33] Mohammad Pezeshki, Diane Bouchacourt, Mark Ibrahim, Nicolas Ballas, Pascal Vincent, and David Lopez-Paz. Discovering Environments with XRM. In *Forty-first International Conference on Machine Learning*, 2024.

[34] Joaquin Quiñonero-Candela, Masashi Sugiyama, Anton Schwaighofer, and Neil D. Lawrence. *Dataset Shift in Machine Learning*. The MIT Press, 12 2008.

[35] Alec Radford, Jong Wook Kim, Chris Hallacy, Aditya Ramesh, Gabriel Goh, Sandhini Agarwal, Girish Sastry, Amanda Askell, Pamela Mishkin, Jack Clark, et al. Learning transferable visual models from natural language supervision. In *International conference on machine learning*, pages 8748–8763. PMLR, 2021.

[36] Ilija Radosavovic, Raj Prateek Kosaraju, Ross B. Girshick, Kaiming He, and Piotr Dollár. Designing network design spaces. In *2020 IEEE/CVF Conference on Computer Vision and Pattern Recognition, CVPR 2020, Seattle, WA, USA, June 13-19, 2020*, pages 10425–10433. Computer Vision Foundation / IEEE, 2020.

[37] Shiori Sagawa, Pang Wei Koh, Tatsunori B. Hashimoto, and Percy Liang. Distributionally robust neural networks. In *International Conference on Learning Representations*, 2020.

[38] Mark Sandler, Andrew G. Howard, Menglong Zhu, Andrey Zhmoginov, and Liang-Chieh Chen. MobileNetV2: Inverted Residuals and Linear Bottlenecks. In *2018 IEEE Conference on Computer Vision and Pattern Recognition, CVPR 2018, Salt Lake City, UT, USA, June 18-22, 2018*, pages 4510–4520. Computer Vision Foundation / IEEE Computer Society, 2018.

[39] Ramprasaath R. Selvaraju, Michael Cogswell, Abhishek Das, Ramakrishna Vedantam, Devi Parikh, and Dhruv Batra. Grad-cam: Visual explanations from deep networks via gradient-based localization. In *IEEE International Conference on Computer Vision, ICCV 2017, Venice, Italy, October 22-29, 2017*, pages 618–626. IEEE Computer Society, 2017.

[40] Karen Simonyan and Andrew Zisserman. Very deep convolutional networks for large-scale image recognition. In Yoshua Bengio and Yann LeCun, editors, *3rd International Conference on Learning Representations, ICLR 2015, San Diego, CA, USA, May 7-9, 2015, Conference Track Proceedings*, 2015.

[41] Sahil Singla and Soheil Feizi. Salient imagenet: How to discover spurious features in deep learning? In *International Conference on Learning Representations*, 2021.

[42] Christian Szegedy, Wei Liu, Yangqing Jia, Pierre Sermanet, Scott E. Reed, Dragomir Anguelov, Dumitru Erhan, Vincent Vanhoucke, and Andrew Rabinovich. Going deeper with convolutions. In *IEEE Conference on Computer Vision and Pattern Recognition, CVPR 2015, Boston, MA, USA, June 7-12, 2015*, pages 1–9. IEEE Computer Society, 2015.

[43] Christian Szegedy, Vincent Vanhoucke, Sergey Ioffe, Jonathon Shlens, and Zbigniew Wojna. Rethinking the inception architecture for computer vision. In *2016 IEEE Conference on Computer Vision and Pattern Recognition, CVPR 2016, Las Vegas, NV, USA, June 27-30, 2016*, pages 2818–2826. IEEE Computer Society, 2016.

[44] Mingxing Tan, Bo Chen, Ruoming Pang, Vijay Vasudevan, Mark Sandler, Andrew Howard, and Quoc V. Le. Mnasnet: Platform-aware neural architecture search for mobile. In *IEEE Conference on Computer Vision and Pattern Recognition, CVPR 2019, Long Beach, CA, USA, June 16-20, 2019*, pages 2820–2828. Computer Vision Foundation / IEEE, 2019.

[45] Mingxing Tan and Quoc V. Le. Efficientnet: Rethinking model scaling for convolutional neural networks. In Kamalika Chaudhuri and Ruslan Salakhutdinov, editors, *Proceedings of the 36th International Conference on Machine Learning, ICML 2019, 9-15 June 2019, Long Beach, California, USA*, volume 97 of *Proceedings of Machine Learning Research*, pages 6105–6114. PMLR, 2019.

[46] Mingxing Tan and Quoc V. Le. Efficientnetv2: Smaller models and faster training. In Marina Meila and Tong Zhang, editors, *Proceedings of the 38th International Conference on Machine Learning, ICML 2021, 18-24 July 2021, Virtual Event*, volume 139 of *Proceedings of Machine Learning Research*, pages 10096–10106. PMLR, 2021.

[47] Zhengzhong Tu, Hossein Talebi, Han Zhang, Feng Yang, Peyman Milanfar, Alan C. Bovik, and Yinxiao Li. Maxvit: Multi-axis vision transformer. In Shai Avidan, Gabriel J. Brostow, Moustapha Cissé, Giovanni Maria Farinella, and Tal Hassner, editors, *Computer Vision - ECCV 2022: 17th European Conference, Tel Aviv, Israel, October 23-27, 2022, Proceedings, Part XXIV*, volume 13684 of *Lecture Notes in Computer Science*, pages 459–479. Springer, 2022.

[48] V.N. Vapnik. An overview of statistical learning theory. *IEEE Transactions on Neural Networks*, 10(5):988–999, 1999.

[49] C. Wah, S. Branson, P. Welinder, P. Perona, and S. Belongie. Caltech-ucsd birds 200. Technical Report CNS-TR-2011-001, California Institute of Technology, 2011.

[50] Catherine Wah, Steve Branson, Peter Welinder, Pietro Perona, and Serge J. Belongie. The Caltech-UCSD Birds-200-2011 Dataset. <https://api.semanticscholar.org/CorpusID:16119123>, 2011.

[51] Jianfeng Wang, Zhengyuan Yang, Xiaowei Hu, Linjie Li, Kevin Lin, Zhe Gan, Zicheng Liu, Ce Liu, and Lijuan Wang. GIT: A Generative Image-to-text Transformer for Vision and Language. *arXiv preprint arXiv:2205.14100*, 2022.

[52] Saining Xie, Ross B. Girshick, Piotr Dollár, Zhuowen Tu, and Kaiming He. Aggregated residual transformations for deep neural networks. In *2017 IEEE Conference on Computer Vision and Pattern Recognition, CVPR 2017, Honolulu, HI, USA, July 21-26, 2017*, pages 5987–5995. IEEE Computer Society, 2017.

[53] Sergey Zagoruyko and Nikos Komodakis. Wide residual networks. In Richard C. Wilson, Edwin R. Hancock, and William A. P. Smith, editors, *Proceedings of the British Machine Vision Conference 2016, BMVC 2016, York, UK, September 19-22, 2016*. BMVA Press, 2016.

[54] Samira Zare and Hien Van Nguyen. Frustratingly Easy Environment Discovery for Invariant Learning. *Computer Sciences & Mathematics Forum*, 9(1), 2024.

[55] Xin Zhang, Yanzhao Zhang, Dingkun Long, Wen Xie, Ziqi Dai, Jialong Tang, Huan Lin, Baosong Yang, Pengjun Xie, Fei Huang, Meishan Zhang, Wenjie Li, and Min Zhang. mGTE: Generalized Long-Context Text Representation and Reranking Models for Multilingual Text Retrieval. *CoRR*, abs/2407.19669, 2024.

[56] Yuhui Zhang, Jeff Z HaoChen, Shih-Cheng Huang, Kuan-Chieh Wang, James Zou, and Serena Yeung. Diagnosing and rectifying vision models using language. *arXiv preprint arXiv:2302.04269*, 2023.

[57] Yuhui Zhang, Jeff Z. HaoChen, Shih-Cheng Huang, Kuan-Chieh Wang, James Zou, and Serena Yeung. Diagnosing and rectifying vision models using language. In *The Eleventh International Conference on Learning Representations, ICLR*, 2023.

[58] Zaiying Zhao, Soichiro Kumano, and Toshihiko Yamasaki. Language-guided Detection and Mitigation of Unknown Dataset Bias, 2024.

Appendix

A Broader impact statement

By systematically detecting a wide spectrum of spuriously correlated concepts, our work stands to enhance the reliability and trustworthiness of AI-driven decisions across various real-world contexts. WASP could help researchers and developers to address unintended consequences that arise when models latch onto misleading data associations, drawing attention to critical responsibilities tied to deploying AI at scale.

B Software and data

We attach the PyTorch [32] implementation of WASP as supplementary material, including a *README.md* file to explain the code, which we will make publicly available. The datasets and pre-trained models used for WASP are already public.

C Limitations

Some limitations of WASP:

- **Concepts vs Input features as SCs.** The learned SCs can be described by our method in relation with the predefined (large set of) concepts, but not directly w.r.t. the input features (e.g. GradCAM [39] like methods).
- **Captioning model used for extracting concepts.** These models usually do not extract all the details in the images, so relying on them limits the concept space, that limits further discovering all SCs from the original images.
- **SCs from a dataset (only) through the lens of a Foundation Model.** While the Foundation Models are usually very robust ones, some SCs (specially those related to low-level - pixel-level - information) can disappear in the high-semantic embedding space of the foundation model, making it impossible for WASP to detect such SCs.
- **Relying on known hierarchies of concepts** The method also relies on known hierarchies of concepts (like WordNet) to filter out concepts related to the desired class. These hierarchies and the relations they provide thus limit the type of filtering that we can ensure.

D Additional related work

Fairness It is important to note that the proposed method can be utilized to evaluate the fairness of a given dataset and that we do conduct benchmarking on the CivilComments dataset, which encompasses racial and religious concerns. However, it is critical to emphasize that our approach is neither designed to measure nor address issues of fairness. Instead, our method is specifically developed to examine whether a given dataset imparts a clear definition of the featured classes to a model — namely, whether classifiers learn spurious correlations and confound class features with environmental features. Accordingly, our work is situated within the literature on subpopulation shift setups and we assess the quality of our proposed approach within this framework. Evaluating our approach on fairness benchmarks lies outside the scope of the current study, but may constitute a subject for subsequent research.

Concept Bottleneck Models Another approach to detecting spurious correlations would be to use models that are interpretable by design, such as Concept Bottleneck Models (CBMs) [18]. CBMs feature a special layer where each neuron’s activations signals the presence or absence of a specific concept within the input sample. This makes it easier to see which concepts are used by the model down the line and also allows a user to filter out the concepts that he may consider as irrelevant for the task at hand. On the downside, CBMs, as proposed by Koh et al. [18], require a human expert to define the set of relevant concepts for each task and also concept-level annotations in a dataset in order to train the concept extraction layer. To circumvent these limitation, Oikarinen et al. [31] use concepts proposed by GPT-3 and then obtain pseudo-labels for those concepts using a CLIP

Table 6: Class names and prompts used in the zero-shot classification task.

	Waterbirds	CelebA	CivilComments
class names	waterbird landbird	non-blonde hair blonde hair	non-offensive offensive
zero-shot prompt	a photo of a {cls}	a photo of a person with {cls}	{cls}
SC-enhanced prompt	a photo of a {cls} in the {SC}	a photo of a {SC} with {cls}	a/an {cls} comment about {SC}

model. This intervention of CBMs on a models’s architecture constrains its reasoning space down to the set of predetermined concepts, yielding, compared to unaltered models, drops in accuracy of up to 4.97%, as reported by Oikarinen et al. [31] in Table 2. Different from this line of works, we never constrain the model in any way, shape or form. What we aim to uncover are SCs learned by general state-of-the-art models used in the industry, which are not explainable by design. Overall both approaches offer a different tradeoff between explainability and expressivity.

E Loss correlation with presence of spuriously correlated concepts

In this experiment, we look at the correlations between the loss values and the concept-to-sample similarities. We compare basic ERM with GroupDRO, applied on groups, that are obtained based on our revealed SCs (and further grouped using the B2T [17] partitioning strategy).

See in Fig. 4 how for GroupDRO, the loss-to-similarity correlation significantly decrease, revealing that the model is less prone to make mistakes on the samples containing SCs. The results show a reduction in correlation scores across all SCs, demonstrating that the revealed groups are relevant to the dataset’s underlying distribution, and can be effectively utilized with specific algorithms to mitigate the model’s dependence on spurious correlations. Fig. 4 shows the Pearson correlation scores after an epoch of training on Waterbirds, on a subset of all SCs.

F SCs and top class-neutral concepts

We present the exhaustive list of SCs found for the Waterbirds (Tab. 11 & 12), CelebA (Tab. 13) and CivilComments (Tab. 14 & 15) datasets. We also present top class-neutral concepts for ImageNet classes. Concept filtering on ImageNet was performed using WordNet relationships alone, without the intervention of a Large Language Model. Accounting for the size of the dataset, we will publish the available data on our repository upon acceptance, and we will restrict the presentation within the context of the current format to a few classes for illustrative purposes in Tab. 24 -17.

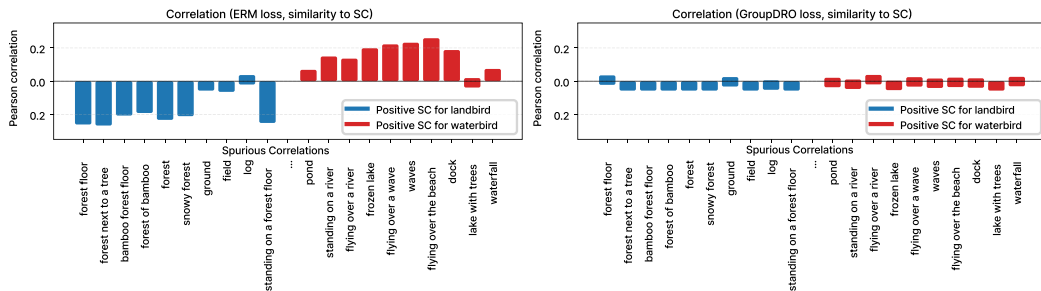


Figure 4: Correlation(sample_loss, sample_to_bias similarity) under ERM/GDRO after one epoch of training on Waterbirds. Loss correlation w/ biases, ERM vs GroupDRO using groups created with the B2T partitioning method. It can be seen that, when training with ERM, loss value is highly correlated with the biases. In contrast, GroupDRO reduces the correlations, intuitively showing that biases discovered with our method are closely related to the ground truth groups of the dataset, being used as shortcuts by the model unless mitigated.

G Zero-Shot Prompts

In Tab. 6, we structured the class names used for initializing the initial weights of the linear layer, along with the prompt templates employed in the zero-shot classification experiments discussed in Sec. 5.1.

H Ablations

We validate several WASP decisions in Tab. 7, for zero-shot classification task, using prompts enhanced with SCs. The number of SCs per class turns out to be very important, taking too many adds noise to the prompts and lowers the performance. Nevertheless, dynamically choosing the threshold, as described in Sec. 3-Step2c., proves to be a good strategy for adapting the cut-off across classes. Following prior observations regarding the modalities gap between text and image embedding space [21, 57], we subtract half of the gap from the embeddings and re-normalize them, ending in marginally lower performance w.r.t. not addressing the gap.

Table 7: Ablation. Following the zero-shot SC-augmented prompting setup, we variate the cut-off threshold for considering causally-unrelated concepts as spuriously correlated and also try to address the text-image modality gap.

Variations	Waterbirds		CelebA		CivilComm	
	(Acc % \uparrow)					
Worst	Avg.	Worst	Avg.	Worst	Avg.	Worst
<i>top-30 candidates</i>	46.3	86.1	66.2	86.4	46.9	71.1
<i>top-20% candidates</i>	46.1	86.0	64.8	86.7	48.8	66.2
<i>modality gap: closed</i>	48.7	85.9	72.7	85.3	-	-
WASP						
* <i>dynamic threshold</i>						
* <i>modality gap: open</i>						
	50.3	86.3	73.1	85.7	53.2	71.0

I Results of state-of-the-art models

We provide results using the same data and experimental setup used for Tables 4 and 5, for an exhaustive list of ImageNet classifiers, in Tables 8, 9 and 10. Pre-trained models together with their respective weight sets are employed from the `torchvision` package.

Table 8: Accuracy of various convolutional and transformer-based models trained on ImageNet-1k, on the data generated for Tab. 4. As with Fig. 2 and Fig. 1, we note that the performance of these models is significantly affected, even though the correct class is clearly illustrated right in front and center while, and the predicted class is absent from the generated images.

Model - Weights	Prompt employed (correct class highlighted in bold, SC in red)			
	a photo of a peafowl	firemen and a peafowl	a photo of a Bernese Mountain Dog	shrimp and pasta near a Bernese Mountain Dog
alexnet - V1 [19]	100.0	4.6	96.2	23.3
convnext_tiny - V1 [25]	100.0	77.2	94.2	69.8
convnext_small - V1 [25]	100.0	92.9	96.3	78.3
convnext_base - V1 [25]	100.0	83.5	99.3	78.0
convnext_large - V1 [25]	100.0	88.2	99.6	81.9
densenet121 - V1 [15]	100.0	52.3	93.1	74.8
densenet161 - V1 [15]	100.0	52.8	84.0	51.6
densenet201 - V1 [15]	100.0	49.7	86.1	80.8
efficientnet_b0 - V1 [45]	100.0	64.5	99.2	92.9
efficientnet_b1 - V1 [45]	100.0	42.6	88.1	67.1
efficientnet_b1 - V2 [45]	100.0	84.2	99.9	69.5
efficientnet_b2 - V1 [45]	100.0	61.7	99.6	82.4
efficientnet_b3 - V1 [45]	100.0	89.1	99.1	92.8
efficientnet_b4 - V1 [45]	100.0	94.4	99.9	72.7
efficientnet_b5 - V1 [45]	100.0	82.9	99.4	86.3
efficientnet_b6 - V1 [45]	100.0	91.2	100.0	95.6
efficientnet_b7 - V1 [45]	100.0	88.3	99.9	90.3
efficientnet_v2_s - V1 [46]	100.0	98.3	99.2	88.1
efficientnet_v2_m - V1 [46]	100.0	95.1	99.8	94.3
efficientnet_v2_l - V1 [46]	100.0	96.0	99.1	83.6
googlenet - V1 [42]	100.0	45.4	95.2	57.0
inception_v3 - V1 [43]	100.0	82.2	98.9	80.8
maxvit_t - V1 [47]	100.0	91.7	99.7	85.3
mnasnet0_5 - V1 [44]	100.0	23.3	96.7	60.8
mnasnet0_75 - V1 [44]	100.0	36.9	98.4	71.1
mnasnet1_0 - V1 [44]	100.0	32.0	89.4	74.9
mnasnet1_3 - V1 [44]	100.0	63.9	91.7	75.6
mobilenet_v2 - V1 [38]	100.0	26.2	84.0	45.0
mobilenet_v2 - V2 [38]	100.0	54.1	98.6	62.8
mobilenet_v3_small - V1 [14]	100.0	16.6	91.0	30.3
mobilenet_v3_large - V1 [14]	100.0	25.4	94.2	23.1
mobilenet_v3_large - V2 [14]	100.0	56.0	96.6	73.7

Table 9: Accuracy of various convolutional and transformer-based models trained on ImageNet-1k, on the data generated for Tab. 4. As with Fig. 1, we note that the performance of these models is significantly affected, even though the correct class is clearly illustrated right in front and center while, and the predicted class is absent from the generated images.

Model - Weights	Prompt employed (correct class highlighted in bold, SC in red)			
	a photo of a peafowl	firemen and a peafowl	a photo of a Bernese Mountain Dog	shrimp and pasta near a Bernese Mountain Dog
regnet_y_400mf - V1 [36]	100.0	35.6	74.7	34.7
regnet_y_400mf - V2 [36]	100.0	72.1	97.7	87.9
regnet_y_800mf - V1 [36]	100.0	22.7	94.8	54.4
regnet_y_800mf - V2 [36]	100.0	81.7	98.9	88.0
regnet_y_1_6gf - V1 [36]	100.0	47.0	96.4	71.7
regnet_y_1_6gf - V2 [36]	100.0	88.2	96.4	74.1
regnet_y_3_2gf - V1 [36]	100.0	33.5	99.4	90.9
regnet_y_3_2gf - V2 [36]	100.0	94.6	98.4	75.4
regnet_y_8gf - V1 [36]	100.0	58.3	71.3	54.8
regnet_y_8gf - V2 [36]	100.0	98.2	96.8	67.5
regnet_y_16gf - V1 [36]	100.0	86.7	97.8	49.8
regnet_y_16gf - V2 [36]	100.0	98.7	91.8	83.5
regnet_y_16gf -				
SWAG_E2E_V1 [36]	100.0	99.6	97.7	78.2
regnet_y_16gf -				
SWAG_LINEAR_V1 [36]	100.0	78.3	100.0	90.7
regnet_y_32gf - V1 [36]	100.0	84.5	99.1	82.3
regnet_y_32gf - V2 [36]	100.0	98.0	99.5	79.6
regnet_y_32gf -				
SWAG_E2E_V1 [36]	100.0	99.6	93.5	71.5
regnet_y_32gf -				
SWAG_LINEAR_V1 [36]	100.0	97.2	100.0	85.6
regnet_y_128gf -				
SWAG_E2E_V1 [36]	100.0	99.6	54.4	67.8
regnet_y_128gf -				
SWAG_LINEAR_V1 [36]	100.0	90.8	99.9	96.9
regnet_x_400mf - V1 [36]	100.0	37.4	82.3	29.0
regnet_x_400mf - V2 [36]	100.0	50.7	99.5	81.7
regnet_x_800mf - V1 [36]	100.0	25.4	77.0	52.6
regnet_x_800mf - V2 [36]	100.0	75.5	97.1	71.4
regnet_x_1_6gf - V1 [36]	100.0	38.2	76.9	66.7
regnet_x_1_6gf - V2 [36]	100.0	82.2	99.2	88.1
regnet_x_3_2gf - V1 [36]	100.0	45.1	62.1	69.4
regnet_x_3_2gf - V2 [36]	100.0	83.4	99.6	88.3
regnet_x_8gf - V1 [36]	100.0	41.8	98.8	89.0
regnet_x_8gf - V2 [36]	100.0	93.5	99.2	81.6
regnet_x_16gf - V1 [36]	100.0	48.7	86.6	54.5
regnet_x_16gf - V2 [36]	100.0	93.4	97.9	88.1
regnet_x_32gf - V1 [36]	100.0	66.1	85.9	46.0
regnet_x_32gf - V2 [36]	100.0	97.4	99.6	83.7
resnet18 - V1 [12]	100.0	36.8	84.3	41.9
resnet34 - V1 [12]	100.0	32.9	54.1	26.1
resnet50 - V1 [12]	100.0	30.1	73.9	54.5
resnet50 - V2 [12]	100.0	80.1	99.7	88.4
resnet101 - V1 [12]	100.0	60.4	92.3	84.4
resnet101 - V2 [12]	100.0	93.4	98.8	87.4
resnet152 - V1 [12]	100.0	66.1	98.4	78.2
resnet152 - V2 [12]	100.0	93.1	98.5	92.5
resnext50_32x4d - V1 [52]	100.0	45.5	92.6	74.8
resnext50_32x4d - V2 [52]	100.0	80.3	98.5	88.0
resnext101_32x8d - V1 [52]	100.0	66.6	84.7	61.2
resnext101_32x8d - V2 [52]	100.0	90.3	99.4	85.2
resnext101_64x4d - V1 [52]	100.0	77.9	97.7	74.2

Table 10: Accuracy of various convolutional and transformer-based models trained on ImageNet-1k, on the data generated for Tab. 4. As with Fig. 2 and Fig. 1, we note that the performance of these models is significantly affected, even though the correct class is clearly illustrated right in front and center while, and the predicted class is absent from the generated images.

Model - Weights	Prompt employed (correct class highlighted in bold, SC in red)				
	a photo of a peafowl	firemen and a peafowl	a photo of a Bernese Mountain Dog	shrimp and pasta near a Bernese Mountain Dog	
shufflenet_v2_x0_5 - V1 [29]	100.0	23.8	36.9	21.0	
shufflenet_v2_x1_0 - V1 [29]	99.8	30.4	72.1	55.9	
shufflenet_v2_x1_5 - V1 [29]	100.0	41.2	97.9	52.5	
shufflenet_v2_x2_0 - V1 [29]	100.0	61.4	99.3	64.5	
squeezeenet1_0 - V1 [16]	100.0	11.4	95.9	28.7	
squeezeenet1_1 - V1 [16]	100.0	13.8	91.2	46.1	
swin_t - V1 [24]	100.0	72.7	96.9	81.6	
swin_s - V1 [24]	100.0	74.3	99.3	81.4	
swin_b - V1 [24]	100.0	81.5	95.2	72.6	
swin_v2_t - V1 [24]	100.0	76.2	88.7	73.6	
swin_v2_s - V1 [24]	100.0	85.7	90.7	74.4	
swin_v2_b - V1 [24]	100.0	73.0	96.0	85.2	
vgg11 - V1 [40]	100.0	9.9	96.6	60.7	
vgg11_bn - V1 [40]	100.0	15.9	86.7	54.8	
vgg13 - V1 [40]	100.0	5.9	97.7	68.1	
vgg13_bn - V1 [40]	100.0	15.5	87.0	13.0	
vgg16 - V1 [40]	100.0	12.2	93.7	66.0	
vgg16_bn - V1 [40]	100.0	22.6	96.1	70.7	
vgg19 - V1 [40]	100.0	26.6	98.5	40.8	
vgg19_bn - V1 [40]	100.0	35.9	83.1	46.2	
vit_b_16 - V1 [9]	100.0	85.4	97.1	75.2	
vit_b_16 - SWAG_E2E_V1 [9]	100.0	88.9	95.8	59.1	
vit_b_16 - SWAG_LINEAR_V1 [9]	100.0	79.2	99.9	84.6	
vit_b_32 - V1 [9]	100.0	56.1	96.0	86.0	
vit_l_16 - V1 [9]	100.0	55.9	95.3	76.0	
vit_l_16 - SWAG_E2E_V1 [9]	100.0	92.1	100.0	93.3	
vit_l_16 - SWAG_LINEAR_V1 [9]	100.0	97.4	100.0	72.5	
vit_l_32 - V1 [9]	100.0	54.0	96.9	82.9	
vit_h_14 - SWAG_E2E_V1 [9]	100.0	99.4	98.5	86.4	
vit_h_14 - SWAG_LINEAR_V1 [9]	100.0	99.7	100.0	96.1	
wide_resnet50_2 - V1 [53]	100.0	60.6	95.7	63.9	
wide_resnet50_2 - V2 [53]	100.0	83.9	99.5	85.4	
wide_resnet101_2 - V1 [53]	100.0	69.3	84.1	72.8	
wide_resnet101_2 - V2 [53]	100.0	91.0	98.8	84.9	

Table 11: Top Waterbirds class-neutral concepts for "landbird".

Landbird	Score
forest floor	0.055562317
forest next to a tree	0.053587496
bamboo forest floor	0.05134508
forest of bamboo	0.04781133
forest	0.047080815
snowy forest	0.044688106
ground	0.043406844
field	0.043168187
log	0.043052554
standing on a forest floor	0.041143
grass covered	0.040526748
tree branch in a forest	0.039670765
forest with trees	0.03949821
tree in a forest	0.039123535
bamboo forest	0.03876221
front of bamboo	0.037381053
mountain	0.036155403
forest of trees	0.03600967
flying through a forest	0.035692394
platform	0.03565806
standing in a forest	0.034528017
hill	0.03341371

Table 12: Top Waterbirds class-neutral concepts for "waterbird".

Waterbird	Score
swimming in the water	0.11482495
water lily	0.10905403
boat in the water	0.1066975
floating in the water	0.106155455
water	0.106134474
flying over the water	0.10561061
standing in the water	0.10444009
sitting in the water	0.103776515
body of water	0.09977633
water in front	0.0902465
standing in water	0.086544394
water and one	0.08424729
swimming	0.07818574
standing on a lake	0.06565446
flying over the ocean	0.06509364
flying over a pond	0.06463468
boats	0.061231434
lifeguard	0.06122452
flying over a lake	0.060126305
boat	0.0571931
pond	0.053261578

Table 13: Top CelebA class-neutral concepts for "non-blonde".

Non-Blonde	Score
hat on and a blue	0.13952243
hat on and a man	0.13853341
man in the hat	0.13803285
man who made	0.13307464
man behind	0.13247031
man with the hat	0.13186401
man is getting	0.12861347
actor	0.12726557
dark	0.12713176
man in a blue	0.1269682
person	0.12541258
man in the blue	0.124844134
man is not a man	0.12308431
man	0.12290484
large	0.1228559
shirt on in a dark	0.12170941
hat	0.121646166
close	0.12146461
man with the blue	0.12136656
man face	0.12130207

Table 14: Top CivilComments class-neutral concepts for "non-offensive".

Non-offensive	Score
allowing	0.07341421
work	0.06982881
made	0.069063246
talk	0.06858361
none are needed	0.067236125
check	0.06664443
helping keep the present	0.06531584
policy	0.06339955
campaign	0.06333798
involved in the first place	0.063222766
Cottage	0.063149124
IDEA	0.06310266
stories	0.0625782
job	0.06236595
allowed	0.062137783
latest news about the origin	0.062061936
giving others who have experienced	0.061925888
proposed	0.061897278
one purpose	0.06122935
starting	0.061154723
small	0.061071455
question	0.060854554
practice	0.060740173
raised	0.060681045
entering	0.060585797
registered	0.060475767
beliefs	0.060165346
accept that they are promoting	0.060070753
Security	0.059328556
new	0.059324086
subject	0.058983028
close	0.058632135
views	0.058573127
Hold	0.058341324
reality for a change	0.058261245
built at that parish	0.057885766
rest	0.057804525
historic	0.057656527
concept	0.057422698
people	0.057151675
passage seems to in reflection	0.05699992
attempt	0.056797385

Table 15: Top CivilComments class-neutral concepts for "offensive".

"Offensive" – Top Concepts	Score
hypocrisy	0.046756804
troll	0.035944045
silly	0.029536605
hate	0.013704538
silly how do you study	0.00325954
spite	0.002645433
kid you have the absolute	0.001619577

Table 16: Top ImageNet class-neutral concepts for "Crossword".

"Crossword" – Top Concepts	Score
reading a newspaper	0.30469692
man reading a newspaper	0.29045385
crochet squares	0.28316277
sitting on a newspaper	0.27749887
newspaper sitting	0.27106437
crochet squares in a square	0.2708223
newspaper that has the words	0.26934764
holding a newspaper	0.26375395
newspaper while sitting	0.26288068
newspaper laying	0.25538272
square with a few crochet	0.2461972
square with a crochet	0.24225119
square of crochet squares	0.23986068
checkerboard	0.23797607
crochet blanket in a square	0.2364017
square of square crochet	0.23590976
on a newspaper	0.2357213
crochet square with a crochet	0.23569846
crochet blanket with a crochet	0.23438567
newspaper	0.23315597
crochet with a square	0.23304509
crochet square	0.23259673
newspaper sitting on	0.23098715
square of crochet yarn	0.2291883
square crochet	0.22903368
crochet blanket with a square	0.22888878
crochet square sitting	0.22860557
crochet in a square	0.22856355
square with a single crochet	0.22752959
free crochet	0.22748157
newspaper with	0.22672665
is on a newspaper	0.2257084
crochet blanket	0.22547376
checkered blanket	0.22514643
square of crochet	0.22324148

Table 17: Top ImageNet class-neutral concepts for "Guacamole".

"Guacamole" – Top Concepts	Score
tomatoes and avocado	0.33948907
avocado	0.3125001
nachos	0.30761188
ham and parsley	0.2960047
with avocado	0.2952027
colorful mexican	0.28313732
bacon and parsley	0.27773544
of avocado	0.2754345
side of salsa	0.27470407
peridot	0.2734925
salsa	0.27124816
nachos with	0.27092364
lime body	0.27088284
cheese and parsley	0.26951405
pile of limes	0.26944226
peas and bacon	0.2671204
limes and limes	0.26682717
lime cut	0.2662533
nachos with and	0.26580203
pasta with peas	0.2626204
tacos	0.2619322
pasta with ham and parsley	0.26183394
tomatoes and cilantro	0.26161948

Table 19: Top ImageNet class-neutral concepts for "Ballpoint Pen".

Table 18: Top ImageNet class-neutral concepts for "Bald Eagle".

"Bald Eagle" – Top Concepts	Score
osprey flying	0.2888234
osprey	0.27377927
row of american flags	0.26513425
group of american flags flying	0.25681192
american flag and american flag	0.23945728
emu standing	0.23752406
yellowstone national	0.23740456

"Ballpoint Pen" – Top Concepts	Score
wearing a pilot	0.36252645
markers	0.36050144
sharpie	0.34563553
stylus	0.34399948
pair of eyeglasses	0.32426757
notepad	0.3228797
calligraphy	0.3222967
paint and markers	0.32198787
close up of a needle	0.32131955
on a straw	0.3209229
and markers	0.32090995
eyeglasses	0.31017447
dots	0.30764964
crayons	0.30598855

Table 20: Top ImageNet class-neutral concepts for "Coffeemaker".

"Coffeemaker" – Top Concepts	Score
kettle sitting on	0.43714887
with a kettle	0.4207235
thermos	0.40833473
kettle	0.40526068
kettle sitting	0.3881535
stovetop maker	0.37747166
kettle kettle	0.37671012
kettle kettle kettle	0.37649006
vases and vases	0.37567452
kettle kettle kettle	0.37547356
flask	0.37485123
kettle kettle kettle kettle	0.37305972
large canister	0.37186915
flasks	0.36940324
decorative vases sitting	0.3683877
kitchen aid	0.36793774
milkshakes	0.36605325
large pottery	0.36506
set of kitchen	0.3650242
cookbook	0.36469316
vases sitting	0.3643943

Table 22: Top ImageNet class-neutral concepts for "Eraser".

"Eraser" – Top Concepts	Score
crayons	0.38733196
chalk	0.37349075
graphite	0.36778685
crayon	0.36178917
charcoal	0.351962
lip balm lip	0.35033816
band aid cookie	0.34825876
lip balm	0.3409983
nose sticking	0.34016216
sticking	0.33971623
markers	0.33940658
matchbox	0.33480892
wand	0.33415005
stylus	0.3318595
band aid card	0.33174193
toothbrush	0.33009088
office supplies	0.32956824
band aid flexible	0.32946587

Table 21: Top ImageNet class-neutral concepts for "Doormat".

"Doormat" – Top Concepts	Score
brick sidewalk	0.37059835
laying on gravel	0.34978455
laying on a carpeted	0.34279323
crochet blanket	0.3421431
sitting on a carpeted	0.34104648
laying on a step	0.3400078
crochet blanket in a square	0.33642814
brick walkway	0.3319164
carpeted floor	0.33067068
on a brick sidewalk	0.32878387
crochet blanket with a crochet	0.32599914
floor with a welcome	0.32548892
square of crochet yarn	0.32428077
crochet blanket made	0.32336423
carpeted staircase	0.3227385
dot blanket	0.3213501
mosaic floor	0.32125634
crocheted blanket	0.31886423
on a blanket	0.3182252
crochet blanket with a square	0.31753486
square of crochet squares	0.3169018
crochet squares	0.3152317
standing in a doorway	0.3126963

Table 23: Top ImageNet class-neutral concepts for "American Lobster".

"American Lobster" – Top Concepts	Score
pasta with shrimp	0.3148532
adirondack sitting	0.31178916
large shrimp	0.3085378
shrimp and pasta	0.30821544
shrimp cooking	0.3032636
large cast cooking	0.30282205
pasta with shrimp and cheese	0.2984723
adirondack	0.29169592
and mussels	0.2904386
legs and other seafood	0.28870153
close up of a shrimp	0.2871693
of pasta with shrimp	0.2823377
seafood	0.2808096
mussels	0.28018713
cast cooking	0.27951774
shrimp and cheese	0.27841187
shrimp	0.2726224

Table 24: Top ImageNet class-neutral concepts for "Fire Truck".

"Fire Truck" – Top Concepts	Score
firefighter spraying	0.34155905
group of firefighters	0.3347583
firefighters	0.33051446
firefighter	0.31450543
firefighter wearing	0.2843979
hydrant spraying	0.26793447
firefighter wearing a	0.26590723
firefighter cuts	0.2613345
farmall parked	0.2591076
dashboard with flames	0.25825307
flames painted	0.2540929